Macromolecules

pubs.acs.org/Macromolecules Article

Mechanochemical Synthesis of Ionic Polymers: Solid-State Ball-Milling Polymerization for Unrestricted Solubility Enabling Copolymerization of Immiscible Monomers

Gue Seon Lee, Hyun Sub Lee, Nuri Kim, Hyun Gyu Shin, Yun Ha Hwang, Seung Jae Lee, and Jeung Gon Kim*

Cite This: *Macromolecules* 2024, 57, 9408−9418 Read Online

ACCESS | Metrics & More | Article Recommendations | Supporting Information

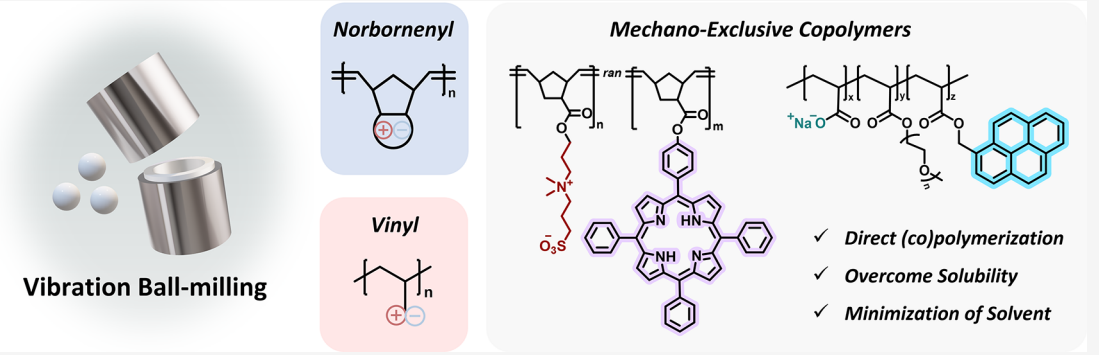

ABSTRACT: This study demonstrates the facile synthesis of ionic polymers using a solid-state mechanochemical ball milling method, which offers a straightforward, ecofriendly, and broad scope compared to conventional solution polymerization techniques. Unlike solution polymerization, which is limited by solvent selection and often results in poor efficiency, direct ball-milling polymerization enables the production of the desired product polymers from a broader range of ionic monomers without solubility and miscibility constraints. We employed free-radical polymerization of styrene and (meth)acrylic ionic monomers, as well as Ru-initiated ring-opening metathesis polymerization of norbornenyl ionic monomers, to demonstrate the effectiveness of the mechanochemical approach. Additionally, the study explored the mechanochemical copolymerization of immiscible monomer pairs such as sodium carboxylate/pyrene and ammonium sulfone betaine/porphyrin moieties, producing water-soluble porphyrin and pyrene polymers. Overall, this research showcases mechanochemistry's versatility and efficiency in synthesizing ionic polymers, anticipating its use in various applications.

1. INTRODUCTION

The synthesis of ionic compounds is limited by their solubility, as they can dissolve only in highly polar solvents. This poses a significant problem when attempting to react ionic compounds with hydrophobic reagents or catalysts, as there is often no common solvent system. The polymerization of ionic monomers exacerbates this issue, as the resulting ionic polymer has an even narrower range of solvents than monomers.[1−4]

In modern polymer science and engineering, especially for biotargeted applications, it is a requisite for materials to operate in water or water-miscible conditions.[5−7] Ionic polymers meet these requirements and have played a crucial role in various fields such as batteries,[8−10] metal-ion removal,[11] nonflammable materials,[12] drug delivery,[13] membranes for oil/water separation,[14] and antimicrobial coatings.[15,16] To improve the performance, we frequently employ copolymerizations. However, immiscibility issues arise when dealing with the copolymerization with hydrophobic monomers. The scope of polymerization methods is further limited when considering other reaction components such as initiators and catalysts. An alternative approach involves postpolymerization modifications, such as quaternization, to introduce ionic functionalities into the polymer structure.[17,18] However, this method requires additional synthetic steps and is limited in incorporating a diverse range of ionic species. Herein, we propose the mechanochemical solid-state direct polymerization of ionic monomers as a solution.

Mechanochemistry is a technique that employs mechanical force to promote chemical transformations.[19,20] Collision or

Received: June 21, 2024
Revised: August 22, 2024
Accepted: September 12, 2024
Published: September 23, 2024

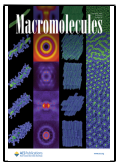

Downloaded via ECOLE POLYTECHNIC FED LAUSANNE on October 23, 2024 at 12:45:39 (UTC).
See https://pubs.acs.org/sharingguidelines for options on how to legitimately share published articles.

© 2024 American Chemical Society

https://doi.org/10.1021/acs.macromol.4c01451
Macromolecules 2024, 57, 9408−9418

Scheme 1. Solid-State Mechanochemical Polymerization of Ionic Monomers

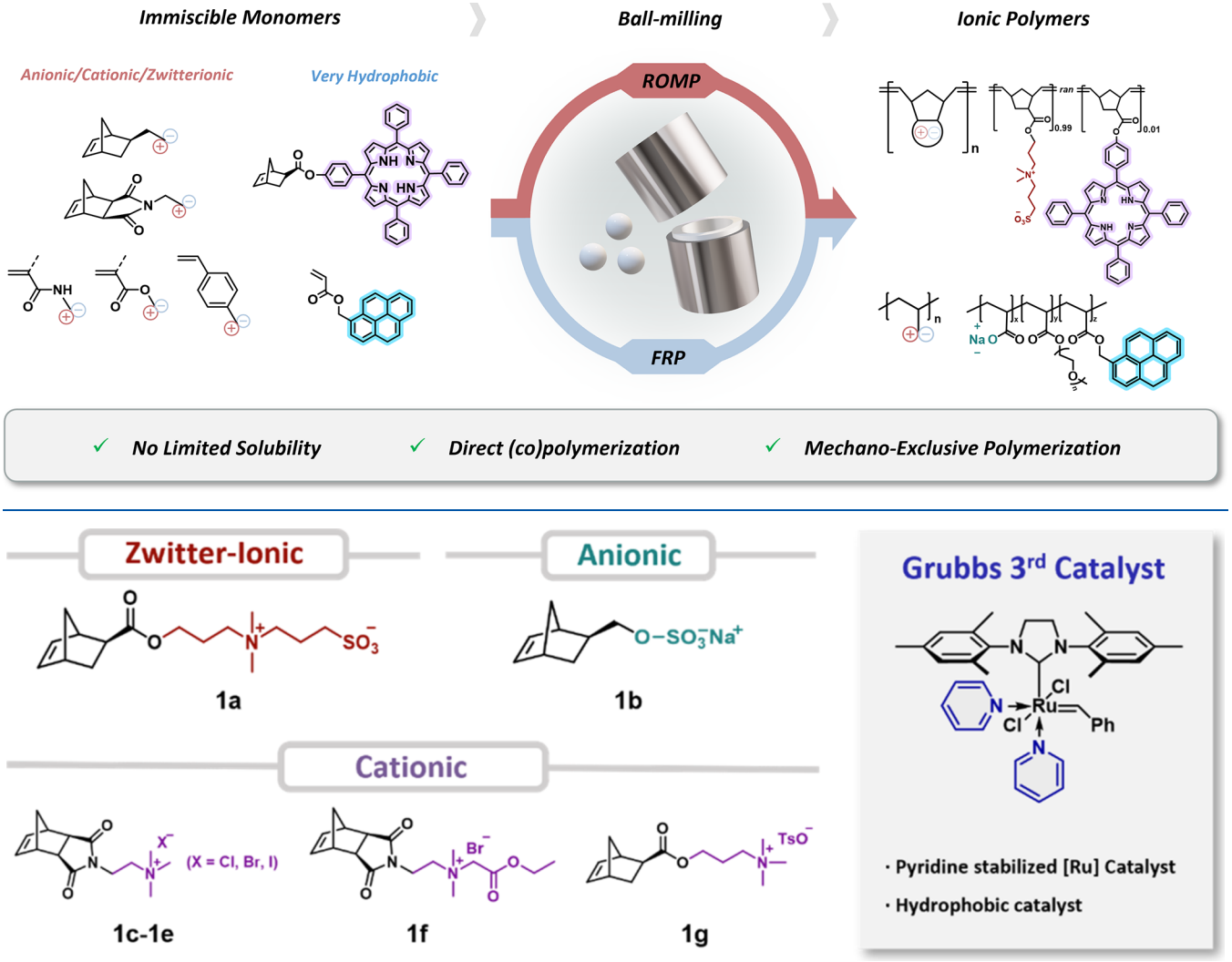

Figure 1. Chemical structure of the ionic norbornenyl monomers **1a−1g** and Grubbs 3rd-generation catalyst (**G3**).

shearing by ball milling or twin screws can provide enough mixing of chemical reagents and activation energy.[21,22] Mechanochemistry has offered solvent-free conditions, energy savings, and increased reactivity.[23−25] Additionally, it has broadened the scope of chemical synthesis, generating exclusive chemical products that are inaccessible under conventional homogeneous solution conditions.[26] For instance, the chemical transformation of poorly soluble materials is possible with ball milling or twin screws.[27,28] Mechanochemistry has also been a solution for the reactions of orthogonally soluble reagents.[29,30] These examples prove that the solubility limit in liquid states does not apply to solid-state mechanochemistry. Narrowing to ionic polymer synthesis, various polymerization techniques have been realized in solid-state ball milling, including radical polymerization of ionic sodium acrylate,[31] mechanoexclusive multiblock copolymer synthesis using heterogeneity of sodium acrylate and acrylamide,[32] and atom transfer radical copolymerization of vinyl styrene and sodium vinyl sulfonate.[33] Recently, our group reported examples of mechanochemical ring-opening metathesis polymerizations (ROMPs) using norbornenes with ammonium sulfone betaine and sodium sulfate.[34]

In this study, we explored the scope of ionomers in mechanochemical polymerizations. Radical polymerizations of vinyl monomers and ROMPs of norbornenyl monomers under ball milling conditions successfully incorporated a wide range of cationic, anionic, and zwitterionic monomers (Scheme 1). Copolymerizing with highly hydrophobic monomers that are incompatible in polar media demonstrates the potential for synthesizing highly functional and mechanoexclusive polymers, thereby advancing copolymer design beyond conventional polymerization methods.

2. RESULTS AND DISCUSSION

2.1. Synthesis of Ionic Homopolymers. *2.1.1. Ru-Alkylidene-Initiated ROMP of Ionic Norbornenes.* ROMP using ruthenium alkylidene is one of the ubiquitous tools in functional polymer synthesis. Especially, chemically robust Ru-carbene scaffolds bear a wide range of functionalities.[35−37] Most Ru-ROMP has been carried out in a single phase with monomers and Ru-alkylidene. Modification has been practiced when polymerizing orthogonally soluble monomers. For ionic polymerization, the ruthenium complex was modified by introducing hydrophilic ligands. For example, the Grubbs group developed a water-soluble ruthenium with a pendant

https://doi.org/10.1021/acs.macromol.4c01451
Macromolecules 2024, 57, 9408−9418

Table 1. Monomer Scope in Mech-ROMP[a,b]

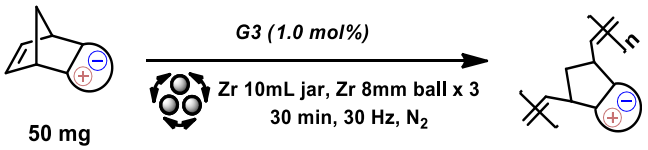

Entry	Monomer	LAG	M_n[c] (kg/mol)	M_w[c] (kg/mol)	$Đ$ [c] (M_w/M_n)	Conv.[d] (%)
1	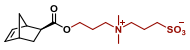	none	4.2	8.4	1.97	85
2	**1a**	H_2O	38.4	58.8	1.53	99
3	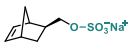	none	N/A	N/A	N/A	< 1
4	**1b**[e]	DMF	46.9	62.7	1.26	99
5	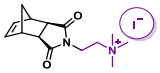	none	N/A	N/A	N/A	9
6	**1c**	DMF	14.1	18.8	1.33	94
7	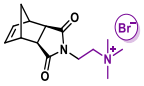	none	3.4	4.1	1.17	31
8	**1d**	DMF	7.6	12.2	1.60	98
9	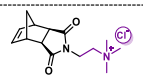	none	2.7	3.3	1.25	39
10	**1e**	DMF	5.4	8.2	1.55	81
11	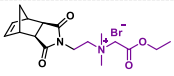	none	N/A	N/A	N/A	22
12	**1f**	H_2O	17.3	22.2	1.29	99
13	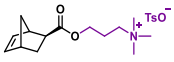	none	3.3	4.1	1.22	88
14	**1g**	H_2O	10.3	14.1	1.37	99

[a]All reactant was loaded into a Zr 10 mL vessel with three Zr 8 mm balls and milled for 30 min at 30 Hz. [b]LAG additive = 20 μL, η = 0.4 [solvent(μL)/ monomer(mg)]. [c]GPC condition for poly**1a** and poly**1b**: 0.03% NaN_3 in H_2O, GPC condition for poly**1c** to poly**1g**: NaOAc 0.50 M/AcOH 10% in H_2O, GPC is calibrated with PEO standards. [d]Conversion was calculated by ^{1}H NMR in D_2O. [e]Milling time = 10 min.

ammonium ionic group[38] and reported ROMP of ionic monomers in 1998.[39] Afterward, ionic monomers were polymerized with various modified ruthenium catalysts in a polar solvent, including methanol, water, trifluoroethanol, and phosphate buffer solution.[40,41] The reports included some copolymerizations but only miscible combinations.

We recently reported an example of mechanochemical ROMP (mech-ROMP) between an ionic monomer and hydrophobic Ru-species, Grubbs third generation catalyst (**G3**).[34] Unmodified **G3** successfully threaded ionic monomers **1a** and **1b** efficiently employing solid-state ball milling, promising a simplified ionic polymer synthesis. Further scope is explored in this report, including cationic, anionic, and zwitterionic moieties (Figure 1 and Table 1).

The study revealed that liquid-assisted grinding (LAG) has a striking effect on mechanochemical ionic ROMP. Neat polymerization of zwitterionic monomer **1a** with an ammonium cation and sulfonate anion exhibited 85% conversion (entry 1); however, the molecular weight just passed an oligomeric range ($M_{n(GPC)}$ = 4.2 kg/mol). We speculated that mechanical chain degradations were severe.[42−44] Previously, our group discovered that LAG can selectively slow down degradations, thus allowing high-molecular weight polymer synthesis.[34,45] The lubrication effect loosened the chain-to-chain interaction; thus, chains could move upon external force and avoid chain scission. LAG with water (20 μL to 50 mg solid) improved the efficiency (99%) and molecular weight ($M_{n(GPC)}$ = 38.4 kg/mol) (Table 1, entry 2).

Polymerization of sulfate monomer **1b** exhibited almost no neat polymerization (entry 3). On the other hand, DMF LAG (20 μL to 50 mg of the solid mixture) promoted the full conversion to the corresponding polymer with a high molecular weight ($M_{n(GPC)}$ = 46.9 kg/mol) (entry 4). We speculated that the strong lattice energy of ionic compounds might not allow contact with **G3**. In addition to the lubrication effect of polymer chains, LAG mitigated an intermolecular interaction, and facile molecular movements provided sufficient mixing of **1b** and **G3**.

Next, we explored the polymerization of quaternary ammonium salts containing norbornene with various counteranions, iodide (**1c**), bromide (**1d**), and chloride (**1e**) (entries 5−10). While all monomers exhibited low conversions under neat conditions, we observed a deviation by anions. Neat polymerization of norbornene with halide counteranions showed lower conversion from chloride to iodide, **1c** (9%, entry 5), **1d** (31%, entry 7), and **1e** (39%, entry 9). The reactivity deviation from that of halide anions on ROMP was

https://doi.org/10.1021/acs.macromol.4c01451
Macromolecules 2024, 57, 9408−9418

Table 2. Molecular Weight Control of Poly1a in Mech-ROMP[a,b]

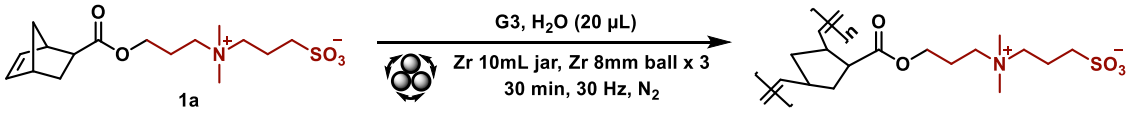

entry	[1a]/[G3]	$M_{w,DOSY}$[c] (kg/mol)	M_n[d] (kg/mol)	M_w[d] (kg/mol)	$Đ$[d] (M_w/M_n)	conv.[e] (%)
1	50	13.4	46.3	77.9	1.69	99
2	100	19.3	38.4	58.8	1.53	99
3	200	44.0	30.9	49.3	1.60	99
4	300	61.5	23.1	35.4	1.53	99

[a]All reactant was loaded into a Zr 10 mL vessel with three Zr 8 mm balls and milled for 30 min at 30 Hz. [b]LAG additive = 20 μL, η = 0.4 [solvent(μL)/ monomer(mg)]. [c]$M_{w,DOSY}$ was obtained by DOSY using PEO standards (see Figure S4). [d]GPC condition: 0.03% NaN_3 in H_2O and PEO standards. [e]Conversion was calculated by ^1H NMR in D_2O.

previously discussed regarding Ru halide exchange reactions. Initial Ru−Cl_2 species undergo fast halide exchange to Ru−Br_2 or Ru−I_2; resulting Ru-complexes exhibited retarded propagation.[46,47] This might affect our observation. The resulting low molecular weights could be due to low efficiency and chain degradation. However, those effects were not vivid under the LAG conditions. LAG with DMF (20 μL to 50 mg solid) improved polymerization efficiency to 94, 98, and 81%. The halide effect was unclear, and **1e** even exhibited the lowest conversion.

To evaluate broad applicability, norbornene monomers containing an ammonium bromide unit in the center of the side chain (**1f**) and a bulky tosylate anion (**1g**) were investigated (entries 11−14). Polymerization of **1f** and **1g** without LAG resulted in lower conversion and molecular weight (entries 11 and 13); water LAG improved conversions to polymers with higher molecular weights ($M_{n(GPC)}$ = 17.3 kg/mol and 10.3 kg/mol, respectively) (entries 12 and 14).

Upon selective retardation of chain degradation by LAG, molecular weight control was anticipated. At [**1a**]/[**G3**] = 50, 100, 200, and 300, poly**1a** was synthesized with the addition of 20 μL of H_2O to 50 mg of **1a** (Table 2). However, GPC measurements showed a decrease in molecular weight at high initiator-to-monomer ratios. We commenced another method to validate polymer molecular weights, diffusion-ordered NMR spectroscopy (DOSY). DOSY provides diffusion coefficients (D) for individual resonances in a ^1H NMR spectrum, offering insights into the hydrodynamic radius of molecules and providing weight-average molecular weight information.[48−50] While GPC depends on the hydrodynamic volume and interaction with column-packing materials,[51−53] DOSY evaluates only hydrodynamic volume in solution conditions.[54−56] The diffusion coefficients of poly**1a** synthesized at various initiator-to-monomer ratios were obtained as D = 4.908 × 10^{-11} to 2.016 × 10^{-11} m^2 s^{-1} in deuterated water (Figure S7). These D values were applied to the viscosity-corrected PEO calibration curve to calculate $M_{w,DOSY}$ (Figure S4).[57] The resulting $M_{w,DOSY}$ of poly**1a** exhibited a linear increase from 13.4 to 61.5 kg/mol (Figure 2). Thus, it confirmed that mechanochemical synthesis of ionic polymers can achieve molecular weight control.

As the ROMP of norbornene monomers with **G3** has been known for well-controlled polymerization, its mechanochemical ionic examples here exhibited a broader dispersity. In addition, we evaluated its block copolymerization of **1a** and **1b**; however, the second block formation was always sluggish. It is important to address the fact that kinetic information derived from solution or liquid states is not entirely valid in solid states. We are currently working on understanding the kinetics of solid polymerization, which would lead to living mech-ROMP.

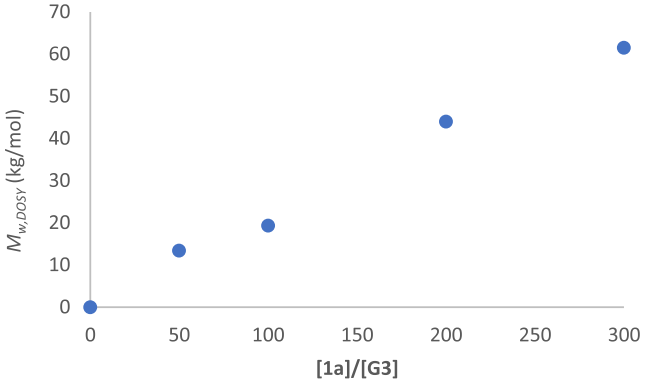

Figure 2. $M_{w,DOSY}$ vs monomer-to-initiator plot.

Further, we evaluated the mechanical impact of comparing high-speed ball milling vs mechanical agitation by a stirring bar (Table S5 and Figure S8). The same reaction mixture as in entry 1, Table 1, was placed in a test tube (10 mL) (Figure S9). A stirring bar rotation (10 mm × 3 mm PTFE spin bar) at 500 rpm produced no polymers, but 1500 rpm stirring for 30 min exhibited 59% conversion. It is difficult to compare the stronger force between high-speed ball milling at 30 Hz and 1500 rpm stirring. Still, we can conclude that the level of mechanical force is directly related to reaction efficiency.

The scalability was checked with a gradual increase to 100, 350, and 500 mg scales. Regardless of the scale, all polymerizations of **1a** exhibited >98% conversions. Molecular weights and dispersity values lay in comparable ranges (50 mg: M_n = 38.4 kg/mol, $Đ$ = 1.53; 100 mg: M_n = 41.6 kg/mol, $Đ$ = 1.29; 350 mg: M_n = 35.7 kg/mol, $Đ$ = 1.28; and 500 mg: M_n = 42.9 kg/mol, $Đ$ = 1.41) (Table S6 and Figure S10).

2.1.2. Free-Radical Polymerization. Mechanochemical radical polymerizations of ionic monomers consisted of the early development of ball-milling polymerizations. The first report by Kargin in 1959 presented sodium acrylate polymerization.[31] Kuzuya's modern study in the 90s investigated the copolymerization of sodium acrylate and acrylamide.[32] Recently, Bielawski reported the copolymerization of sodium styrenesulfonate and 1-vinyl naphthalene.[33] In this report, we commenced a scope study on free-radical mechanochemical polymerizations with a series of ionic monomers that have styrenic and (meth)acrylic groups (Figure 3).

https://doi.org/10.1021/acs.macromol.4c01451
Macromolecules 2024, 57, 9408−9418

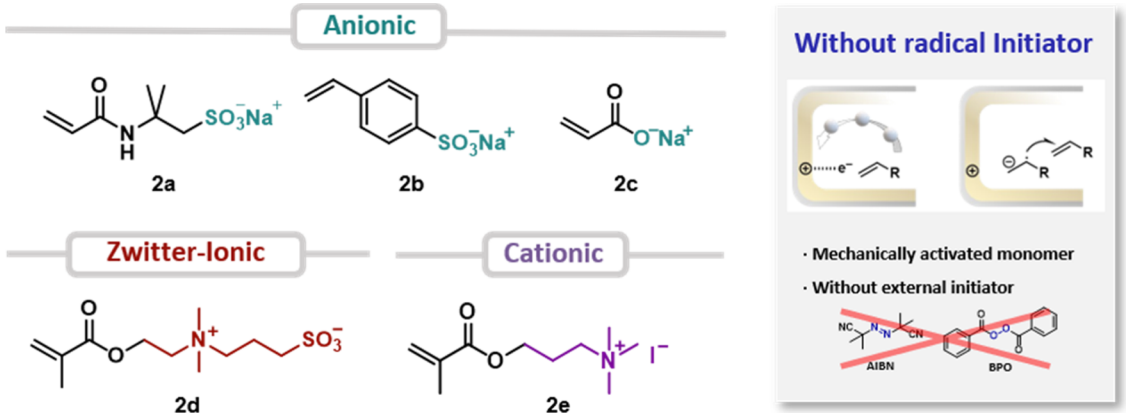

Figure 3. Chemical structure of ionic vinyl monomers **2a**–**2e**.

Table 3. Monomer Scope in Radical Polymerization[a,b]

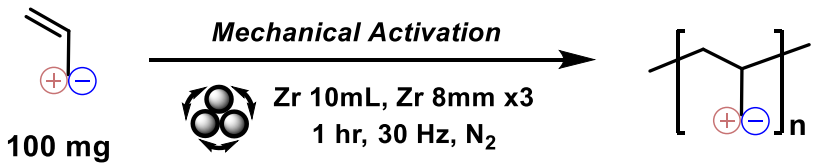

Entry	Monomer	LAG	M_n[c] (kg/mol)	M_w[c] (kg/mol)	$Đ$[c] (M_w/M_n)	Conv.[d] (%)
1	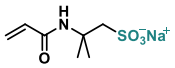	none	42.8	47.7	1.12	98
2	**2a**	H_2O	> limit	> limit	> limit	99
3	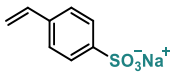	none	50.6	53.7	1.06	90
4	**2b**	H_2O	52.8	71.5	1.35	12
5	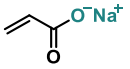	none	33.2	37.7	1.13	99
6	**2c**	H_2O	> limit	> limit	> limit	83
7	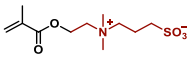	none	54.5	62.9	1.16	97
8	**2d**	H_2O	> limit	> limit	> limit	99
9	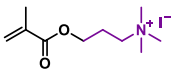	none	4.2	4.8	1.13	97
10	**2e**	H_2O	7.5	11.1	1.46	77

[a]Zr 10 mL vessel with three Zr 8 mm balls, 1 h at 30 Hz. [b]LAG additive = 40 μL, η = 0.4 [solvent(μL)/ monomer(mg)]. [c]GPC condition for poly**2a** to poly**2d**: 0.03% NaN_3 in H_2O, GPC condition for poly**2e**: NaOAc 0.50 M/AcOH 10% in H_2O, and GPC was calibrated with PEO standards. [d]Conversion was calculated by ^{1}H NMR in D_2O.

High-impact energy can polymerize activated vinyl monomers directly without an external initiator.[20,58−60] Self-initiation of monomers or electron transfer from the collision of jars and balls would promote radical polymerizations. We successfully synthesized ionic polymers by introducing 100 mg of the monomer into the milling vessel (Zr 10 mL) with three balls (Zr 8 mm) and vibration for an hour at 30 Hz (Table 3).

Neat polymerization of sulfonate monomers (**2a** and **2b**), possessing an acrylamide- and styrene-based structure, was successfully achieved (entries 1 and 3). Both monomers exhibited good efficiency over 90% conversions and high molecular weight compared to the PEO standard ($M_{n(GPC)}$ = 42.8 and 50.6 kg/mol, respectively). When polymerized with the addition of water (40 μL to 100 mg of solid), monomer **2a** exhibited an extremely high molecular weight, surpassing a GPC standard limit (entry 2). However, the DOSY measurement of poly**2a** showed $M_{w,DOSY}$ = 4.6 kg/mol (neat) and $M_{w,DOSY}$ = 16.5 kg/mol (LAG), which were significantly lower than the GPC data (Table S8 and Figure S12). The molecular weight from GPC seemed to be overestimated due to fast

https://doi.org/10.1021/acs.macromol.4c01451
Macromolecules 2024, 57, 9408−9418

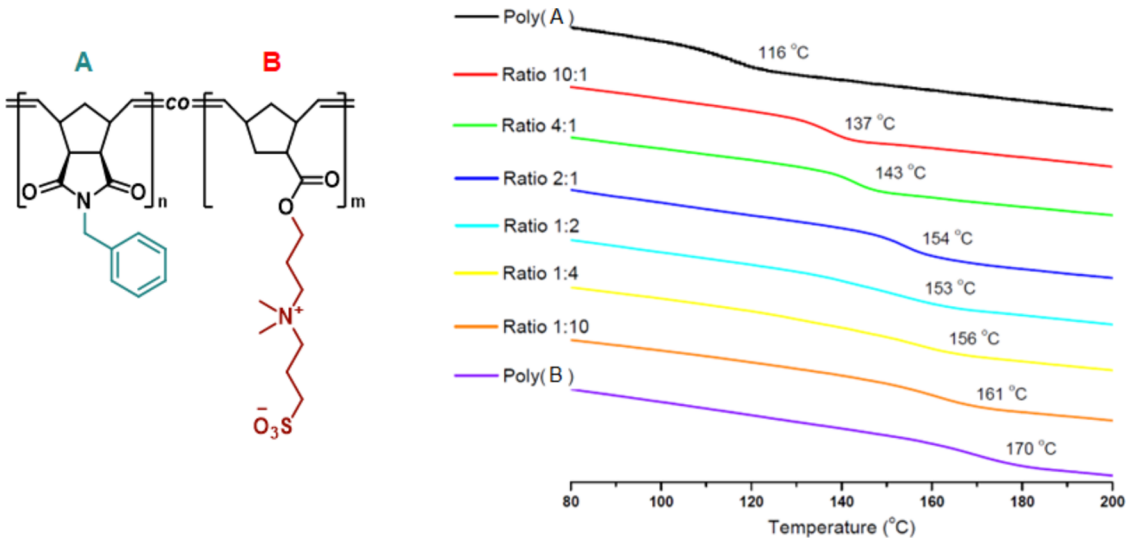

Figure 4. DSC curve and T_g values according to monomer compositions (reproduced from ref 34. with permission from the Royal Society of Chemistry).

Table 4. Copolymerization of Immiscible Monomers[a]

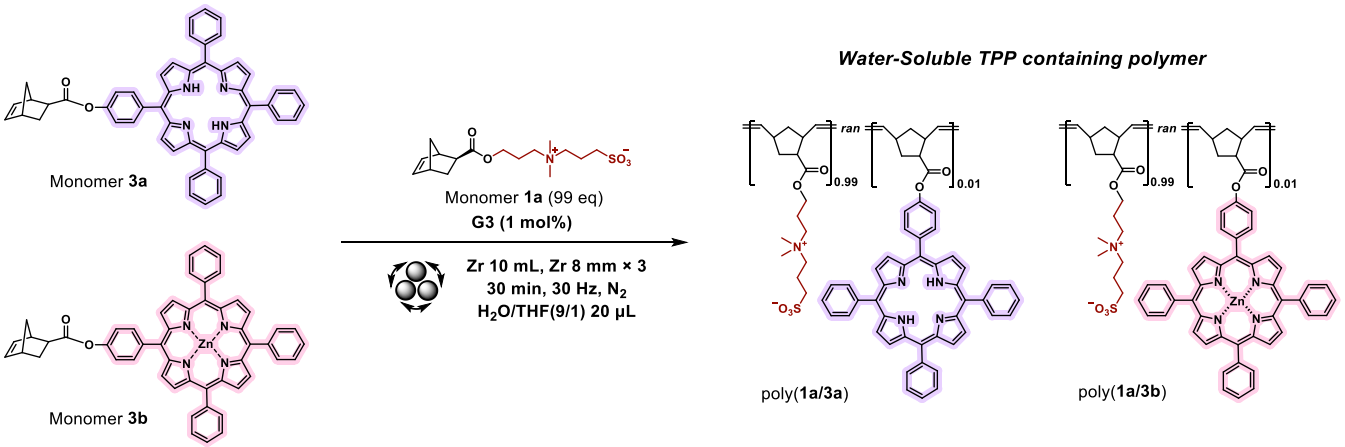

entry	copolymer[b]	solvent[c]	M_n[d] (kg/mol)	M_w[d] (kg/mol)	$Đ$[d] (M_w/M_n)	conv. of **1a**[e] (%)
1	poly(**1a**/**3a**)	THF/H_2O (9/1)	36.5	51.2	1.41	99
2	poly(**1a**/**3b**)	THF/H_2O (9/1)	21.9	28.7	1.31	99

[a]All reactant was loaded into a Zr 10 mL vessel with three Zr 8 mm balls and milled for 30 min at 30 Hz. [b][**1a**/**3a**] = 99/1 and [**1a**/**3b**] = 99/1, total monomer mass = 50 mg, 1 mol % of **G3**. [c]20 μL of THF/H_2O = 9/1 mixture was used as a LAG solvent, η= 0.4 [solvent(μL)/monomer(mg)]. [d]GPC condition: 0.03% NaN_3 in H_2O. [e]Conversion was calculated by ^{1}H NMR in D_2O.

elution caused by repulsive interactions with the negatively charged GPC column. These results confirmed that chain degradation is severe under neat conditions and that LAG alleviated it. Conversely, styrene-based monomer **2b** demonstrated a reduced conversion (12%) compared to the neat grinding product (entry 4); its cause is unclear at this moment. The carboxylate **2c**, ammonium sulfone betaine **2d**, and ammonium monomers **2e** were also assessed through polymerization with or without liquid assistance (entries 5−10). The resulting polymers obtained by adding water demonstrated higher molecular weights than those obtained by neat grinding, indicating the effectiveness of LAG in achieving higher polymerization levels by preventing chain degradation. Overall, mechanochemical free-radical polymerization exhibited unexpectedly low dispersity compared to conventional ones. It is unclear at this point due to the lack of kinetic information on initiation, propagation, termination, and chain degradation steps under solid conditions.

2.2. Copolymerization of Immiscible Pairs. *2.2.1. Copolymerization of Norbornenyl Ammonium Sulfone Betaine/Porphyrin Monomers.* Conventional polymerization has limitations in the range of copolymers because it is affected by the solubility of the monomers. On the other hand, solubility issues in mechanochemistry can be neglected.[33] Our previous study investigated the copolymerization of norbornene derivatives containing a hydrophilic ammonium sulfone betaine monomer and a hydrophobic benzyl monomer.[34] Our findings demonstrated that molecular-level mixing was achieved. Single glass transition temperature (T_g) was observed and dictated the copolymer compositions (Figure 4). The single T_g implied that there are no locally populated block-type units and two orthogonal monomers are statistically distributed. Further, we attempted to copolymerize highly

https://doi.org/10.1021/acs.macromol.4c01451
Macromolecules 2024, 57, 9408−9418

hydrophobic porphyrin norbornene with ionic norbornene, expecting water-soluble porphyrin-containing polymers.

The direct copolymerization of ammonium sulfone betaine **1a** (99 equiv) and either tetraphenyl porphyrin (TPP) **3a** (1 equiv) or zinc-coordinated TPP (Zn-TPP) **3b** (1 equiv) was realized in the ball-milling setup with **G3** (1 mol %) (Table 4). Contrary to the homopolymerization of **1a**, a different LAG composition, H_2O/THF = 9:1, was used. It exhibited better porphyrin incorporation than using only H_2O (Figure S15). The resulting polymers exhibited molecular weights comparable to those of homopolymer poly**1a** ($M_{n,poly(1a/3a)}$ = 36.5 kg/mol and $M_{n,poly(1a/3b)}$ = 21.9 kg/mol vs $M_{n,poly1a}$ = 38.4 kg/mol). The incorporation of porphyrin units was confirmed by ultraviolet−visible spectroscopy (UV−vis) measurements in water (Figure 5). While the water-insoluble porphyrin monomers have no UV−vis signal in water (Figure S19), the copolymers, poly(**1a**/**3a**) and poly(**1a**/**3b**), exhibited typical UV−vis absorption patterns of porphyrins in water. The absorption peaks at 380−400 nm (Soret band) and four peaks at 450−700 nm (Q-band) confirmed TPP and Zn-TPP units of poly(**1a**/**3a**) and poly(**1a**/**3b**). Upon increasing the organic solvent (THF), ionic polymers became insoluble (Figure 6). As the portion of THF increased, the polymer solution became cloudy (Figure 6a), which resulted in a decrease in UV−vis absorption intensity (Figure 6b).

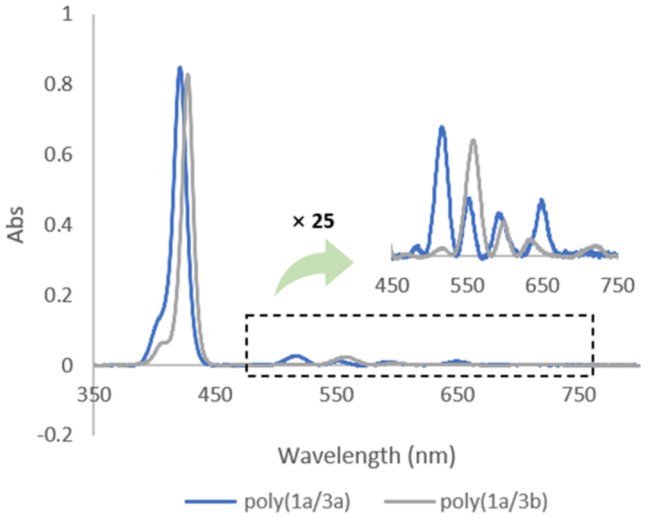

Figure 5. UV−vis absorption spectra of poly(**1a**/**3a**) and poly(**1a**/**3b**) (conc.: 10 mg/mL in H_2O).

Next, we evaluated the efficiency of mech-ROMP compared to solution-based ROMP in the copolymerization of immiscible monomers (Table S10). A mixture of monomers **1a** and **3a** in 99:1 molar ratio was dissolved in water and methanol, targeting 0.5 M concentration. While monomer **1a** exhibited good solubility in both solvents, **3a** showed only a slight solubility in methanol, indicated by the pale-reddish color of the solution (Figure S17). Interestingly, hydrophobic catalyst **G3** facilitated rapid polymerization of **1a** in both solvents. However, the significantly reduced UV absorption of the polymer product from the water solvent indicated poor incorporation of hydrophobic **3a** in water owing to insolubility (Figure S18). In contrast, the copolymer synthesized in methanol displayed a UV absorption intensity comparable to that of the mech-ROMP product, suggesting better incorporation of **3a**. However, GPC revealed the advantage of mech-ROMP. The poly(**1a**/**3a**) copolymer synthesized in methanol showed a bimodal molecular weight distribution, whereas the product from mech-ROMP exhibited an unimodal distribution (Figures S13 and S16). This difference was attributed to the quick precipitation of polymer products during polymerization in methanol, leading to uneven kinetic profiles. Facile synthesis of the water-soluble porphyrin-containing polymer was realized in mechanochemical methods, and its application under physiologically relevant conditions is currently under investigation.[61,62]

2.2.2. Incorporation of Pyrene into the Hydrogel. We employed mechanochemical free-radical polymerization to embrace the hydrophobic pyrene moiety into the ionic-polymer gel. Three monomers, sodium acrylate **2c** (100 mg, 98 equiv), pyrene acrylate **3c** (6.3 mg, 2 equiv), and poly(ethylene glycol) diacrylate cross-linker (24.3 mg, 2 mol %), with 40 μL of H_2O/THF(9/1) mixture were directly copolymerized

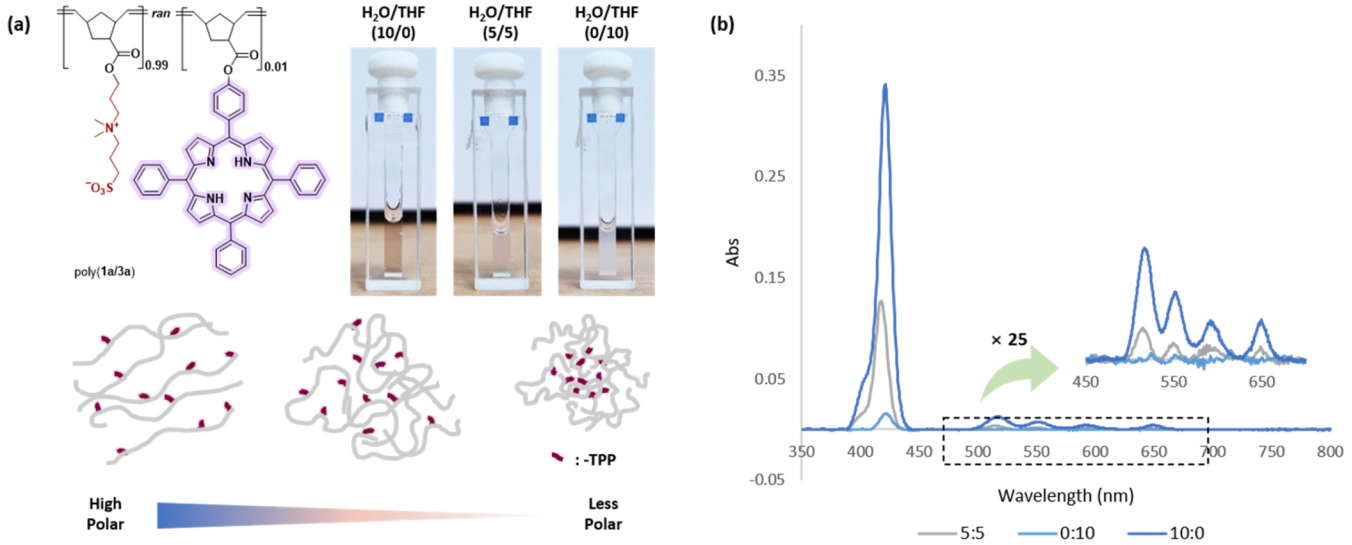

Figure 6. (a) Photographic images of cuvette cells according to solvent mixture ratios and predicted image of polymer chain coagulation depending on the solubility. (b) UV−vis absorption spectrum of poly(**1a**/**3a**) differing in the H_2O/THF ratio (conc.: 10 mg/mL).

https://doi.org/10.1021/acs.macromol.4c01451
Macromolecules 2024, 57, 9408−9418

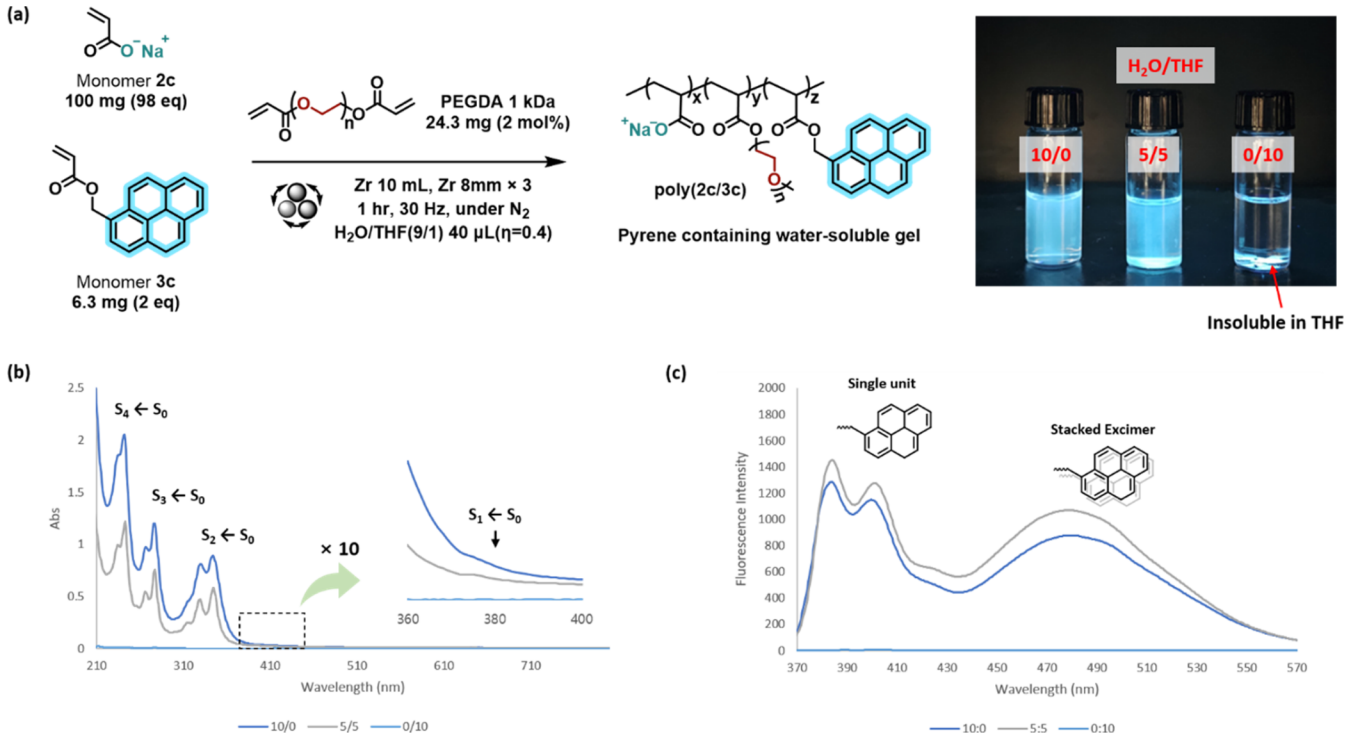

Figure 7. (a) Mechanochemical synthesis of the water-soluble pyrene-containing polymer gel and photographic emission images of poly(**2c**/**3c**) upon UV radiation under various solvent mixture ratios. (b) UV−vis absorption spectra of poly(**2c**/**3c**) differing in the H_2O/THF ratio (1 mg/mL in a solvent mixture). (c) Fluorescent emission spectra of poly(**2c**/**3c**) differing in the H_2O/THF ratio (360 nm excitation, 1 mg/mL in a solvent mixture).

without an initiator (Figure 7). We conducted polymerization using H_2O as the sole LAG solvent; however, the incorporation of pyrene was significantly lower compared to that of the H_2O/THF mixture (Figure S22). The crude product, soluble in water, underwent purification through dialysis in deionized water. Upon dissolving the obtained polymer in water and subjecting it to UV irradiation at 365 nm, we observed the emission of blue light throughout the solution (Figure 7a). Further absorption and fluorescence spectral studies of poly(**2c**/**3c**) were conducted under varying H_2O and THF ratios. Four absorption peaks attributed to pyrene were identified in UV−vis (Figure 7b).[63,64] Subsequently, the absorption intensity decreased as the proportion of the relatively hydrophobic THF increased. In the emission study, the fluorescence spectrum displayed distinct single pyrene emission peaks at 385 and 402 nm and an excimer emission peak at 480 nm simultaneously with excitation at 360 nm (Figure 7c). This implies that a portion of hydrophobic pyrenes are aggregated in a hydrophilic polymer network, while some pyrene units are placed solely. As the THF ratio increased to 50%, a slight increase in fluorescence intensity was detected from both a single unit and a stacked excimer. However, in pure THF, poly(**2c**/**3c**) was insoluble, leading to the inability to detect any emission peaks. These copolymer pyrene/ionic monomers exhibit applications at the fluorescent sensor in aqueous medium, organic electronics, and graphene or carbon nanotube dispersion via $\pi-\pi$ interactions with pyrene.[65−68]

3. CONCLUSIONS

Through the utilization of mechanochemistry, this study pioneers a novel approach to synthesize ionic polymers, offering a sustainable and efficient alternative to conventional solution-based methods. By employing solid-state ball-milling ROMP and radical polymerization, we successfully synthesized ionic homopolymers and mechanoexclusive copolymers, overcoming solubility limitations and enabling the incorporation of diverse monomers. The versatility of this method was exemplified through copolymerizing immiscible monomer pairs and integrating hydrophobic functional groups, such as porphyrin and pyrene, into water-soluble ionic polymers. In addition, LAG offered a chance for high-molecular weight polymer synthesis and molecular weight control by selectively limiting chain degradations. This study emphasizes the pivotal role of mechanochemistry in advancing polymer synthesis methodologies, offering avenues for future research and development.

4. EXPERIMENTAL SECTION

4.1. General Information. All solvents were obtained as high-performance liquid chromatography (HPLC) grade and dried over preactivated 3 Å molecular sieves and neutral alumina. Sodium 4-vinylbenzenesulfonate (90% technical grade, Alfa Aesar) and 2-acrylamido-2-methyl-1-propanesulfonic acid sodium salt solution (in water, 50 wt %, Sigma-Aldrich) were dissolved in water and purified by precipitation in acetone. After filtration, the monomer powder was dried by a freeze dryer for 1 day. Other reagents from commercial sources were used without further purification. All polymerization experiments were prepared under a nitrogen atmosphere using a glovebox. Then, the assembled jar was transferred to a Retsch Mixer Mill MM 400 instrument for designated ball milling. The milling was conducted in a thermostated container at 30 °C to minimize the outer temperature effect.

4.2. Instruments. ^{1}H NMR and ^{1}H DOSY spectra were obtained by using a Bruker AVANCE III HD-400 MHz Fourier transform NMR spectrometer at the Future Energy Convergence Core Center

https://doi.org/10.1021/acs.macromol.4c01451
Macromolecules 2024, 57, 9408−9418

(FECC). ^{1}H DOSY experiments were performed with reference to the following paper.[57] All ^{1}H DOSY experiments were run without spinning to avoid convection. The poly(ethylene oxide) (PEO) standards were prepared at 1 mg/mL in D_2O. ^{1}H DOSY spectra were measured at 298 K with the ledbpgp2s pulse program using 2 spoil gradients. Pulse gradients were used with a relaxation delay (D1) of 30 s. The number of gradient steps (TD) was set to 32. Before measuring 2D-DOSY, two separate 1D-DOSY experiments are measured with the set gradient pulse at minimum (2%) and maximum (95%) gradient strengths. The pulse strength (P_{30} = 1000 to 3000 us) and diffusion time (D_{20} = 0.05 to 0.5 s) were adjusted so that the difference in the minimum/maximum gradient strength was 20 to 50 times. After completing the 2D-DOSY experiment, Topspin 3.6.4 was used for data acquisition and processing. The GPC system was composed of a Waters 2414 differential refractive index detector, a Waters 1515 isocratic pump, and a column heating module to determine the relative number-average molecular weight (M_n) and the weight-average molecular weight (M_w). Aqueous system GPC: Shodex GF-510HQ columns were eluted with an HPLC-grade solvent at 40 °C and 1.0 mL/min. A calibration curve was obtained with 12 monodispersed poly(ethylene oxide) standards (Agilent, EasyCal). UV spectroscopy studies were performed in H_2O or THF at 0.001 to 10 mg/mL using 10 mm-path length quartz cuvettes with Teflon stoppers using a Varian Cary 3500 UV−vis spectrophotometer equipped with a compact Peltier apparatus. Fluorescence spectroscopy studies were carried out in H_2O or THF at 1 mg/mL using an FP8300 spectrofluorometer (JASCO) and cuvettes (JASCO J/3 type, material Q 10 mm × 10 mm).

4.2.1. Representative Procedures of Mechanochemical Ring-Opening Metathesis Polymerization. A monomer was added to a ZrO_2 milling vessel (10 mL) with 8 mm ZrO_2 balls (3 ea). The **G3** stock solution in THF was added to the top closure. This part was left for 1 min to allow the THF to evaporate, leaving the designated amount of **G3**. The LAG solvent (20 μL, η = 0.4) was added to the milling vessel. The main vessel and top closure were assembled. The assembled milling apparatus was placed on the MM 400 and milled for 30 min, at 30 Hz in a thermostat at 30 °C. The milling apparatus was opened and a few drops of ethyl vinyl ether were added to quench the polymerization. The polymer powder inside the container was dissolved by adding water and collecting it three times using water. Afterward, a few drops of the crude product were collected, and NMR and GPC analyses were performed to determine the conversion and molecular weights.

4.2.2. Mechanochemical Free-Radical Polymerization. Monomer and the LAG solvent (H_2O 40 μL, η = 0.4) were added to a ZrO_2 milling vessel (10 mL) with 8 mm ZrO_2 balls (3 ea). The main vessel and top closure were assembled. The assembled milling apparatus was placed on the MM 400 and milled for 60 min at 30 Hz in a thermostat at 30 °C. The milling apparatus was opened and quenched with air. The polymer powder inside the container was dissolved by adding water and collecting it three times using water. Afterward, a few drops of the crude product were collected, and NMR and GPC analyses were performed to determine the conversion and molecular weights.

■ ASSOCIATED CONTENT

Supporting Information

The Supporting Information is available free of charge at https://pubs.acs.org/doi/10.1021/acs.macromol.4c01451.

Synthesis of the monomer, GPC curve of polymers, and spectral characterization of the monomer and polymer (PDF)

■ AUTHOR INFORMATION

Corresponding Author

Jeung Gon Kim − *Department of Chemistry, Jeonbuk National University, Jeonju 54896, Republic of Korea; Research Institute of Physics and Chemistry and Department of JBNU-KIST Industry-Academia Convergence Research, Jeonbuk National University, Jeonju 54896, Republic of Korea;* orcid.org/0000-0003-1685-2833; Email: jeunggonkim@jbnu.ac.kr

Authors

Gue Seon Lee − *Department of Chemistry, Jeonbuk National University, Jeonju 54896, Republic of Korea*

Hyun Sub Lee − *Department of Chemistry, Jeonbuk National University, Jeonju 54896, Republic of Korea*

Nuri Kim − *Department of Chemistry, Jeonbuk National University, Jeonju 54896, Republic of Korea*

Hyun Gyu Shin − *Department of Chemistry, Jeonbuk National University, Jeonju 54896, Republic of Korea*

Yun Ha Hwang − *Department of Chemistry, Jeonbuk National University, Jeonju 54896, Republic of Korea*

Seung Jae Lee − *Department of Chemistry, Jeonbuk National University, Jeonju 54896, Republic of Korea; Institute of Molecular Biology and Genetics, Jeonbuk National University, Jeonju 54796, Republic of Korea;* orcid.org/0000-0001-9471-6808

Complete contact information is available at: https://pubs.acs.org/10.1021/acs.macromol.4c01451

Notes

The authors declare no competing financial interest.

■ ACKNOWLEDGMENTS

This research was supported by the National Research Foundation of Korea (2022R1A6A3A13064356 and RS-2024-00342198) and the Samsung Science & Technology Foundation (SRFC-MA1902-05).

■ REFERENCES

(1) Lobb, E. J.; Ma, I.; Billingham, N. C.; Armes, S. P.; Lewis, A. L. Facile Synthesis of Well-Defined, Biocompatible Phosphorylcholine-Based Methacrylate Copolymers via Atom Transfer Radical Polymerization at 20 °C. *J. Am. Chem. Soc.* **2001**, *123* (32), 7913−7914.

(2) Wang, H.; Hirano, T.; Seno, M.; Sato, T. Radical polymerization behavior of 3-(*N*-2-methacryloyloxyethyl-*N*,*N*-dimethyl) ammonato-propanesulfonate in water. *Eur. Polym. J.* **2003**, *39* (11), 2107−2114.

(3) Laschewsky, A.; Zerbe, I. Polymerizable and polymeric zwitterionic surfactants: 1. Synthesis and bulk properties. *Polymer* **1991**, *32* (11), 2070−2080.

(4) Lee, W. F.; Tsai, C. C. Synthesis and solubility of the poly (sulfobetaine)s and the corresponding cationic polymers: 1. Synthesis and characterization of sulfobetaines and the corresponding cationic monomers by nuclear magnetic resonance spectra. *Polymer* **1994**, *35* (10), 2210−2217.

(5) Church, D. C.; Davis, E.; Caparco, A. A.; Takiguchi, L.; Chung, Y. H.; Steinmetz, N. F.; Pokorski, J. K. Polynorbornene-Based Bioconjugates by Aqueous Grafting-from Ring-Opening Metathesis Polymerization Reduce Protein Immunogenicity. *Cell Rep. Phys. Sci.* **2022**, *3* (10), No. 101067.

(6) Wright, D. B.; Touve, M. A.; Thompson, M. P.; Gianneschi, N. C. Aqueous-Phase Ring-Opening Metathesis Polymerization-Induced Self-Assembly. *ACS Macro Lett.* **2018**, *7* (4), 401−405.

(7) Zhao, S.; Huang, W.; Wang, C.; Wang, Y.; Zhang, Y.; Ye, Z.; Zhang, J.; Deng, L.; Dong, A. Screening and Matching Amphiphilic Cationic Polymers for Efficient Antibiosis. *Biomacromolecules* **2020**, *21* (12), 5269−5281.

(8) Shin, J. C.; Lee, A. R.; Shim, J.; Lee, M. Cyclic Ammonium-Based Polyester Ionenes: Chemical Structures and Properties for Electrochemical Applications. *ACS Appl. Polym. Mater.* **2023**, *5* (12), 9776−9784.

(9) Luo, G.; Yuan, B.; Guan, T.; Cheng, F.; Zhang, W.; Chen, J. Synthesis of Single Lithium-Ion Conducting Polymer Electrolyte Membrane for Solid-State Lithium Metal Batteries. *ACS Appl. Energy Mater.* **2019**, *2* (5), 3028−3034.
(10) Paulsen, B. D.; Tybrandt, K.; Stavrinidou, E.; Rivnay, J. Organic mixed ionic-electronic conductors. *Nat. Mater.* **2020**, *19* (1), 13−26.
(11) Chowdhury, N.; Solaiman; Roy, C. K.; Firoz, S. H.; Foyez, T.; Imran, A. B. Role of Ionic Moieties in Hydrogel Networks to Remove Heavy Metal Ions from Water. *ACS Omega* **2021**, *6* (1), 836−844.
(12) Kolhe, S. M.; Kumar, A. Radiation-induced grafting of vinyl benzyl trimethyl ammonium chloride onto nylon-6 fabric. *Radiat. Phys. Chem.* **2007**, *76* (5), 901−906.
(13) Sun, H.; Chang, M. Y. Z.; Cheng, W. I.; Wang, Q.; Commisso, A.; Capeling, M.; Wu, Y.; Cheng, C. Biodegradable Zwitterionic Sulfobetaine Polymer and Its Conjugate with Paclitaxel for Sustained Drug Delivery. *Acta Biomater.* **2017**, *64*, 290−300.
(14) Joo, M.; Shin, J.; Kim, J.; You, J. B.; Yoo, Y.; Kwak, M. J.; Oh, M. S.; Im, S. G. One-Step Synthesis of Cross-Linked Ionic Polymer Thin Films in Vapor Phase and Its Application to an Oil/Water Separation Membrane. *J. Am. Chem. Soc.* **2017**, *139* (6), 2329−2337.
(15) Zhou, F.; Qin, X. S.; Li, Y. C.; Ren, L. X.; Zhao, Y. H.; Yuan, X. Y. Fluorosilicone multiblock copolymers tethering quaternary ammonium salt groups for antimicrobial purpose. *Appl. Surf. Sci.* **2015**, *347* (30), 231−241.
(16) Schönemann, E.; Koc, J.; Karthauser, J. F.; Ozcan, O.; Schanzenbach, D.; Schardt, L.; Rosenhahn, A.; Laschewsky, A. Sulfobetaine Methacrylate Polymers of Unconventional Polyzwitterion Architecture and Their Antifouling Properties. *Biomacromolecules* **2021**, *22* (4), 1494−1508.
(17) Zhu, Y.; Noy, J.-M.; Lowe, A. B.; Roth, P. J. The synthesis and aqueous solution properties of sulfobutylbetaine (co)polymers: comparison of synthetic routes and tuneable upper critical solution temperatures. *Polym. Chem.* **2015**, *6* (31), 5705−5718.
(18) Se, K.; Kijima, M.; Ohtomo, R.; Fujimoto, T. Quaternization of poly(tertiary aminostyrene)s and characterization of the quaternized polymers. *J. Polym. Sci., Part A: Polym. Chem.* **1997**, *35* (7), 1219−1226.
(19) Hernández, J. G.; Bolm, C. Altering Product Selectivity by Mechanochemistry. *J. Org. Chem.* **2017**, *82* (8), 4007−4019.
(20) Krusenbaum, A.; Grätz, S.; Tigineh, G. T.; Borchardt, L.; Kim, J. G. The mechanochemical synthesis of polymers. *Chem. Soc. Rev.* **2022**, *51* (7), 2873−2905.
(21) Zholdassov, Y. S.; Yuan, L.; Garcia, S. R.; Kwok, R. W.; Boscoboinik, A.; Valles, D. J.; Marianski, M.; Martini, A.; Carpick, R. W.; Braunschweig, A. B. Acceleration of Diels-Alder reactions by mechanical distortion. *Science* **2023**, *380* (6649), 1053−1058.
(22) Bolt, R. R. A.; Leitch, J. A.; Jones, A. C.; Nicholson, W. I.; Browne, D. L. Continuous flow mechanochemistry: reactive extrusion as an enabling technology in organic synthesis. *Chem. Soc. Rev.* **2022**, *51* (11), 4243−4260.
(23) Park, S.; Kim, J. G. Mechanochemical synthesis of poly(trimethylene carbonate)s: an example of rate acceleration. *Beilstein J. Org. Chem.* **2019**, *15* (1), 963−970.
(24) Thorwirth, R.; Bernhardt, F.; Stolle, A.; Ondruschka, B.; Asghari, J. Switchable selectivity during oxidation of anilines in a ball mill. *Chem. - Eur. J.* **2010**, *16* (44), 13236−13242.
(25) Oh, C.; Choi, E. H.; Choi, E. J.; Premkumar, T.; Song, C. Facile Solid-State Mechanochemical Synthesis of Eco-Friendly Thermoplastic Polyurethanes and Copolymers Using a Biomass-Derived Furan Diol. *ACS Sustainable Chem. Eng.* **2020**, *8* (11), 4400−4406.
(26) Cuccu, F.; De Luca, L.; Delogu, F.; Colacino, E.; Solin, N.; Mocci, R.; Porcheddu, A. Mechanochemistry: New Tools to Navigate the Uncharted Territory of "Impossible" Reactions. *ChemSusChem* **2022**, *15* (17), No. e202200362.
(27) Seo, T.; Toyoshima, N.; Kubota, K.; Ito, H. Tackling solubility issues in organic synthesis: solid-state cross-coupling of insoluble aryl halides. *J. Am. Chem. Soc.* **2021**, *143* (16), 6165−6175.
(28) Cao, Q.; Crawford, D. E.; Shi, C.; James, S. L. Greener Dye Synthesis: Continuous, Solvent-Free Synthesis of Commodity Perylene Diimides by Twin-Screw Extrusion. *Angew. Chem.* **2020**, *132* (11), 4508−4513.
(29) Cho, J.; Shin, J.; Kang, M.; Verwilst, P.; Lim, C.; Yoo, H.; Kim, J. G.; Zhang, X.; Hong, C. S.; Kim, J. S.; Kim, S. Calix[*n*]triazolium based turn-on fluorescent sensing ensemble for selective adenosine monophosphate (AMP) detection. *Chem. Commun.* **2021**, *57* (91), 12139−12142.
(30) Kim, N.; Go, E. S.; Kim, J. G. Mechanochemical indium(0)-mediated Barbier allylation of carbonyl compounds: unexpected immiscible water additive effect for hydrophobic reagents. *RSC Mechanochem.* **2024**, *1* (2), 158−161.
(31) Kargin, V. A.; Plate, N. A. Chemical grafting on crystal surfaces. *Vysokomol. Soed.* **1959**, *1*, No. 330.
(32) Kondo, S.-i.; Hatakeyama, I.; Hosaka, S.; Kuzuya, M. Mechanochemical solid-state polymerization (X): the influence of copolymer structure in copolymeric prodrugs on the nature of drug release. *Chem. Pharm. Bull.* **2000**, *48* (12), 1882−1885.
(33) Cho, H. Y.; Bielawski, C. W. Atom Transfer Radical Polymerization in the Solid-State. *Angew. Chem.* **2020**, *132* (33), 14033−14039.
(34) Lee, G. S.; Lee, H. W.; Lee, H. S.; Do, T.; Do, J.-L.; Lim, J.; Peterson, G. I.; Friščić, T.; Kim, J. G. Mechanochemical ring-opening metathesis polymerization: development, scope, and mechano-exclusive polymer synthesis. *Chem. Sci.* **2022**, *13* (39), 11496−11505.
(35) Samojłowicz, C.; Bieniek, M.; Grela, K. Ruthenium-Based Olefin Metathesis Catalysts bearing N-Heterocyclic Carbene Ligands. *Chem. Rev.* **2009**, *109* (8), 3708−3742.
(36) Hilf, S.; Kilbinger, A. F. M. Thiol-Functionalized ROMP Polymers via Sacrificial Synthesis. *Macromolecules* **2009**, *42* (12), 4127−4133.
(37) McQuade, J.; Serrano, M. I.; Jäkle, F. Main Group Functionalized Polymers through Ring-Opening Metathesis Polymerization (ROMP). *Polymer* **2022**, *246*, No. 124739.
(38) Mohr, B.; Lynn, D. M.; Grubbs, R. H. Synthesis of water-soluble, aliphatic phosphines and their application to well-defined ruthenium olefin metathesis catalysts. *Organometallics* **1996**, *15* (20), 4317−4325.
(39) Lynn, D. M.; Mohr, B.; Grubbs, R. H. Living Ring-Opening Metathesis Polymerization in Water. *J. Am. Chem. Soc.* **1998**, *120* (7), 1627−1628.
(40) Isarov, S. A.; Pokorski, J. K. Protein ROMP: Aqueous Graft-from Ring-Opening Metathesis Polymerization. *ACS Macro Lett.* **2015**, *4* (9), 969−973.
(41) Foster, J. C.; Varlas, S.; Blackman, L. D.; Arkinstall, L. A.; O'Reilly, R. K. Ring-Opening Metathesis Polymerization in Aqueous Media Using a Macroinitiator Approach. *Angew. Chem., Int. Ed.* **2018**, *57* (33), 10672−10676.
(42) Peterson, G. I.; Ko, W.; Hwang, Y.-J.; Choi, T.-L. Mechanochemical Degradation of Amorphous Polymers with Ball-Mill Grinding: Influence of the Glass Transition Temperature. *Macromolecules* **2020**, *53* (18), 7795−7802.
(43) Jung, E.; Yim, D.; Kim, H.; Peterson, G. I.; Choi, T. L. Depolymerization of poly (*α*-methyl styrene) with ball-mill grinding. *J. Polym. Sci.* **2023**, *61* (7), 553−560.
(44) Jung, E.; Cho, M.; Peterson, G. I.; Choi, T. L. Depolymerization of Polymethacrylates with Ball-Mill Grinding. *Macromolecules* **2024**, *57* (7), 3131−3137.
(45) Ohn, N.; Shin, J.; Kim, S. S.; Kim, J. G. Mechanochemical Ring-Opening Polymerization of Lactide: Liquid-Assisted Grinding for the Green Synthesis of Poly(lactic acid) with High Molecular Weight. *ChemSusChem* **2017**, *10* (18), 3529−3533.
(46) Rankin, D. A.; P'Pool, S. J.; Schanz, H. J.; Lowe, A. B. The controlled homogeneous organic solution polymerization of new hydrophilic cationic exo-7-oxanorbornenes via ROMP with $RuCl_2(PCy3)_2CHPh$ in a novel 2,2,2-trifluoroethanol/methylenechloride solvent mixture. *J. Polym. Sci., Part A: Polym. Chem.* **2007**, *45* (11), 2113−2128.

https://doi.org/10.1021/acs.macromol.4c01451
Macromolecules 2024, 57, 9408−9418

(47) Sanford, M. S.; Love, J. A.; Grubbs, R. H. Mechanism and Activity of Ruthenium Olefin Metathesis Catalysts. *J. Am. Chem. Soc.* **2001**, *123* (27), 6543−6554.
(48) Ruzicka, E.; Pellechia, P.; Benicewicz, B. C. Polymer Molecular Weights via DOSY NMR. *Anal. Chem.* **2023**, *95* (20), 7849−7854.
(49) Nelson, T. F.; Ward, C. P. Diffusion-Ordered spectroscopy for rapid and facile determination of consumer plastic molecular weight. *Anal. Chem.* **2023**, *95* (22), 8560−8568.
(50) Groves, P. Diffusion ordered spectroscopy (DOSY) as applied to polymers. *Polym. Chem.* **2017**, *8* (44), 6700−6708.
(51) Volet, G.; Lesec, J. Non-exclusion effects in aqueous SEC: behavior of some polyelectrolytes using on-line mass detectors. *J. Liq. Chromatogr.* **1994**, *17* (3), 559−577.
(52) Colak, S.; Tew, G. N. Dual-Functional ROMP-Based Betaines: Effect of Hydrophilicity and Backbone Structure on Nonfouling Properties. *Langmuir* **2012**, *28* (1), 666−675.
(53) Huang, F.; Hou, L.; Wu, H.; Wang, X.; Shen, H.; Cao, W.; Yang, W.; Cao, Y. High-efficiency, environment-friendly electroluminescent polymers with stable high work function metal as a cathode: Green-and yellow-emitting conjugated polyfluorene polyelectrolytes and their neutral precursors. *J. Am. Chem. Soc.* **2004**, *126* (31), 9845−9853.
(54) Li, W. B.; Chung, H. Y.; Daeffler, C.; Johnson, J. A.; Grubbs, R. H. Application of ^{1}H DOSY for facile measurement of polymer molecular weights. *Macromolecules* **2012**, *45* (24), 9595−9603.
(55) Gu, K. C.; Onorato, J.; Xiao, S. S. Y. S.; Luscombe, C. K.; Loo, Y. L. Determination of the molecular weight of conjugated polymers with diffusion-ordered NMR spectroscopy. *Chem. Mater.* **2018**, *30* (3), 570−576.
(56) Montgomery, J. R. D.; Lancefield, C. S.; Miles-Barrett, D. M.; Ackermann, K.; Bode, B. E.; Westwood, N. J.; Lebl, T. Fractionation and DOSY NMR as Analytical Tools: From Model Polymers to a Technical Lignin. *ACS Omega* **2017**, *2* (11), 8466−8474.
(57) Voorter, P.; Mckay, A.; Dai, J.; Paravagna, O.; Cameron, N. R.; Junkers, T. Solvent-Independent Molecular Weight Determination of Polymers Based on a Truly Universal Calibration. *Angew. Chem., Int. Ed.* **2022**, *61* (5), No. e202114536.
(58) Simionescu, C. I.; Oprea, C. V.; Nicoleanu, J. Mechanochemically initiated polymerizations-5. Polymerization by vibratory milling of acrylamide and methacrylamide. *Eur. Polym. J.* **1983**, *19* (6), 525−528.
(59) Kuzuya, M.; Kondo, S. I.; Noguchi, A. A new development of mechanochemical solid-state polymerization of vinyl monomers: prodrug syntheses and its detailed mechanistic study. *Macromolecules* **1991**, *24* (14), 4047−4053.
(60) Hu, C.; van Bonn, P.; Demco, D. E.; Bolm, C.; Pich, A. Mechanochemical synthesis of stimuli responsive microgels. *Angew. Chem.* **2023**, *135* (34), No. e202305783.
(61) Pathak, P.; Zarandi, M. A.; Zhou, X.; Jayawickramarajah, J. Synthesis and Applications of Porphyrin-Biomacromolecule Conjugates. *Front. Chem.* **2021**, *9*, No. 764137.
(62) Zhuo, C.; You, H.; Gao, F.; Liu, S.; Wang, X.; Wang, F. Bottlebrush polymeric catalyst: Boosting activity for CO2/epoxide copolymerization. *Fuel* **2023**, *333*, No. 126434.
(63) Crawford, A. G.; Dwyer, A. D.; Liu, Z.; Steffen, A.; Beeby, A.; Pålsson, L.-O.; Tozer, D. J.; Marder, T. B. Experimental and theoretical studies of the photophysical properties of 2- and 2,7-functionalized pyrene derivatives. *J. Am. Chem. Soc.* **2011**, *133* (34), 13349−13362.
(64) Feng, X.; Wang, X.; Redshaw, C.; Tang, B. Z. Aggregation Behaviour of Pyrene-Based Luminescent Materials, from Molecular Design and Optical Properties to Application. *Chem. Soc. Rev.* **2023**, *52* (19), 6715−6753.
(65) Shen, P.; Jiang, Z.; Viktorova, J.; Pollard, B.; Kumar, A.; Stachurski, Z.; Connal, L. A. Conductive and Self-Healing Carbon Nanotube−Polymer Composites for Mechanically Strong Smart Materials. *ACS Appl. Nano Mater.* **2023**, *6* (2), 986−994.
(66) Odaci, D.; Gacal, B. N.; Gacal, B.; Timur, S.; Yagci, Y. Fluorescence Sensing of Glucose Using Glucose Oxidase Modified by PVA-Pyrene Prepared via "Click" Chemistry. *Biomacromolecules* **2009**, *10* (10), 2928−2934.
(67) Xue, C. H.; Zhou, R. J.; Shi, M. M.; Gao, Y.; Wu, G.; Zhang, X. B.; Chen, H. Z.; Wang, M. The Preparation of Highly Water-Soluble Multi-Walled Carbon Nanotubes by Irreversible Noncovalent Functionalization with a Pyrene-Carrying Polymer. *Nanotechnology* **2008**, *19* (21), No. 215604.
(68) Alosime, E. M. A Review on Surface Functionalization of Carbon Nanotubes: Methods and Applications. *Discover Nano* **2023**, *18* (1), No. 12.

https://doi.org/10.1021/acs.macromol.4c01451
Macromolecules 2024, 57, 9408−9418